

# Efficient unitary preparation of non-trivial quantum states

Wen Wei Ho<sup>1</sup> and Timothy H. Hsieh<sup>2,3</sup>

<sup>1</sup>*Department of Physics, Harvard University, Cambridge, Massachusetts 02138, USA*

<sup>2</sup>*Kavli Institute for Theoretical Physics, University of California, Santa Barbara, California 93106, USA*

<sup>3</sup>*Perimeter Institute for Theoretical Physics, Waterloo, Ontario N2L 2Y5, Canada*

(Dated: May 13, 2022)

We provide a route for preparing non-trivial quantum states that are not adiabatically connected to unentangled product states. Specifically, we find explicit unitary circuits which *exactly* prepare (i) the Greenberger-Horne-Zeilinger (GHZ) state, (ii) a quantum critical ground state, and (iii) a topologically ordered ground state, all with circuit depth  $O(L)$ , where  $L$  is the linear dimension of the system. We obtain these circuits both numerically, using a variant of the ‘Quantum Approximate Optimization Algorithm’ (QAOA) [E. Farhi et al., [arXiv:1411.4028](https://arxiv.org/abs/1411.4028)], and analytically, in the case of GHZ and topological order. Our results are practically useful for achieving non-trivial states in synthetic quantum systems and illustrate the utility of QAOA-type circuits as variational wavefunctions for non-trivial phases of matter.

*Introduction.* – Recent experimental advances in designing and controlling well-isolated synthetic many-body systems, for example trapped ions [1, 2], Rydberg atom arrays [3], ultracold atoms [4] and superconducting qubits [5, 6], have allowed for a whole host of interesting physics to be studied. These include both equilibrium and out-of-equilibrium phenomena like topological order [7–9], phase transitions [10, 11], thermalization [12, 13], and also novel nonequilibrium phases of matter such as time crystals [14, 15]. Equally exciting is the potential to use these platforms for the purposes of performing quantum simulations or computation [3, 6, 16] or for speed-ups in quantum metrology precision measurements, utilizing many-body entanglement [17–20].

For the above purposes of exploring non-trivial many-body phases of matter and enabling quantum information protocols, the ability to prepare complex quantum states is vital. Many protocols require access to states with non-trivial patterns of entanglement and which are not adiabatically connected to short-range entangled states. For example, proposals for speed-ups in quantum many-body metrology measurements [17–20] require the Greenberger-Horne-Zeilinger (GHZ) state, and measurement-based quantum computing requires highly entangled initial states [21–23]. Therefore, it is important to have explicit, resource-efficient schemes for preparing non-trivial quantum states.

The quantum adiabatic algorithm (QAA) [24, 25] is one candidate method: the ground state of a desired Hamiltonian can be prepared from that of an easily accessible Hamiltonian by slowly tuning the interaction parameters, so that at any instance the system remains in the ground state manifold. However, while physically intuitive, the QAA is not the ‘most efficient’ one for state preparation: there are works that introduce counterdiabatic terms which minimize diabatic transitions to improve the algorithm [26–29]. Moreover, the Pontryagin principle [30–33] in optimal control theory tells us that the optimal protocol should actually be a ‘bang-

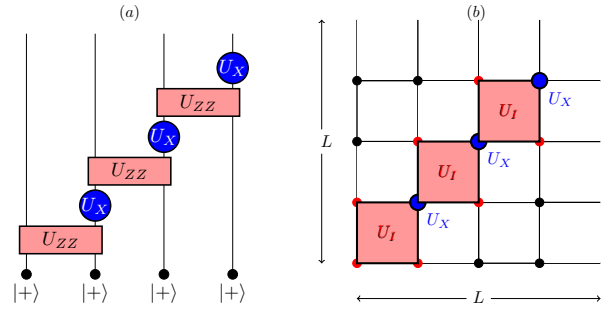


Figure 1. Depth- $2(L - 1)$  quantum circuits used to transform a product state into (a) the GHZ state: here  $U_{ZZ} = e^{\frac{i\pi}{4} Z_i Z_{i+1}}$ ,  $U_X = e^{\frac{i\pi}{4} X_i}$ ; and (b) a topologically ordered state. Here  $U_I$  is evolution of the Wen-plaquette interaction for time  $\pi/4$ .  $U_{I,X}$  are applied one by one, in similar alternating fashion as the GHZ circuit. We have shown an application of the circuit along a particular diagonal only (top-down view); other diagonals can be acted on in parallel.

bang’ type, where the Hamiltonian is abruptly switched between extremal values within the allowed control parameters. In such a case, the working principle is rather different from that of the adiabatic algorithm [34].

The ‘Quantum Approximate Optimization Algorithm’ (QAOA), recently introduced by Farhi et al. [35, 36], is one such example of a ‘bang-bang’ protocol. First proposed as a way of approximately preparing ground states of classical Hamiltonians that encode solutions to certain difficult combinatorial problems, the QAOA (and variants) also provides variational wavefunctions for strongly correlated many-body systems [37] and serves as a promising hybrid approach of coupling near-term quantum computers with optimization on a classical computer to tackle many-body problems.

In this Letter, we use both QAOA as well as analytic methods to construct quantum circuits which efficiently prepare three important classes of non-trivial

many-body states (GHZ, quantum critical, and topologically ordered states) from unentangled product states. These states are hard to prepare from a QAA point of view as the initial and target states constitute different phases of matter; during the dynamical evolution, the system must encounter a gap closing, leading to transitions out of the instantaneous ground state manifold. The QAOA, not requiring adiabaticity in principle, potentially allows a more effective route to prepare nontrivial quantum states.

As a proof of concept, we find protocols that prepare with *perfect* fidelity both the GHZ state and the critical state of the 1d transverse field Ising model of size  $L$  with minimum time that scales as  $t \sim O(L)$ . The fact that one can achieve perfect fidelity in the preparation of a critical ground state illustrates that indeed, the QAOA has a rather different working principle from the QAA. Moreover, we find analytically a simple, explicit quantum circuit to prepare exactly a ground state of the 2d toric code of linear dimension  $L$  with time that also goes as  $t \sim O(L)$ , see fig. 1. Our results provide practical roadmaps for achieving non-trivial states in synthetic quantum systems and illustrate the utility of QAOA-type circuits for the purpose of non-trivial state preparation.

*Non-trivial quantum states.* – Consider a target state  $|\psi_t\rangle$  and an unentangled product state  $|\psi_u\rangle$ , both defined on a system with linear dimension  $L$ . We define  $|\psi_t\rangle$  to be non-trivial if there does not exist a local unitary circuit  $U$  of finite depth ( $\sim O(L^0)$ ), or equivalently, a local Hamiltonian evolving for a time  $t \sim \mathcal{O}(L^0)$  that connects the two:  $|\psi_t\rangle = U|\psi_u\rangle$  [38]. Instead, the depth of any local unitary circuit that connects the two must be at least  $O(L^\alpha)$  with  $\alpha > 0$ . Intuitively, nontrivial states have entanglement structures fundamentally different from product states. Note that this is a statement made without reference to the notion of a gap or Hamiltonian.

We now review why the GHZ, critical, and topologically ordered states are nontrivial. Suppose there exists a local unitary  $U$  of finite depth that takes the completely polarized product state  $|+\rangle \equiv \otimes |X = 1\rangle$  to the GHZ state  $|\text{GHZ}\rangle \equiv \frac{1}{\sqrt{2}}(\otimes |Z = 1\rangle + \otimes |Z = -1\rangle)$ . ( $X, Z$  are Pauli operators). Due to locality, there exists a Lieb-Robinson bound which limits the spread of information and entanglement under this evolution, implying that the finite depth circuit can only generate a finite correlation length  $\xi$  for the final state. Measuring a long-range spin-spin correlation function in the GHZ state gives  $\langle \text{GHZ} | Z_i Z_j | \text{GHZ} \rangle = 1$  while on the other hand the same quantity can be expressed as

$$\begin{aligned} \langle + | U^\dagger Z_i U U^\dagger Z_j U | + \rangle &\xrightarrow{|i-j| \gg \xi} \langle + | U^\dagger Z_i U | + \rangle \langle + | U^\dagger Z_j U | + \rangle \\ &= \langle \text{GHZ} | Z_i | \text{GHZ} \rangle \langle \text{GHZ} | Z_j | \text{GHZ} \rangle = 0, \end{aligned} \quad (1)$$

which is a contradiction. Similar arguments apply to critical states which have power-law correlations and topo-

logically ordered states which have long-range correlations in loop operators (as well as non-zero topological entanglement entropy) [39–42]. From the perspective of Hamiltonians and energy gaps, such states are separated from product states by a gap-closing phase transition in the thermodynamic limit, and thus preparing them with the QAA is hard.

*QAOA.* – The QAOA begins with an easily prepared state  $|\psi_u\rangle$  such as the ground state  $|+\rangle$  of a paramagnet  $H_X = -\sum_i X_i$ . We then act on the state by sequentially alternating between an interaction Hamiltonian  $H_I$  (usually taken to be the Hamiltonian of interest whose ground state we hope to achieve, but this can be tweaked) and the paramagnet  $H_X$  for a total of  $p$  times, so that the resulting state is

$$|\psi(\vec{\gamma}, \vec{\beta})\rangle_p = e^{-i\beta_p H_X} e^{-i\gamma_p H_I} \dots e^{-i\beta_1 H_X} e^{-i\gamma_1 H_I} |+\rangle. \quad (2)$$

We call such a protocol  $\text{QAOA}_p$ . The depth of the above circuit, which counts the number of times either the  $H_I$  or  $H_X$  unitaries are applied, is  $2p$ . The angles (or times)  $(\vec{\gamma}, \vec{\beta}) \equiv (\gamma_1, \dots, \gamma_p, \beta_1, \beta_p)$  are to be found by optimizing some cost function  $F_p(\vec{\gamma}, \vec{\beta})$ , such as the energy expectation value of the target Hamiltonian:

$$F_p(\vec{\gamma}, \vec{\beta}) = {}_p\langle \psi(\vec{\gamma}, \vec{\beta}) | H_I | \psi(\vec{\gamma}, \vec{\beta}) \rangle_p, \quad (3)$$

and the state corresponding to these optimal angles is therefore the optimal state that can be prepared by the protocol given this cost function. The QAOA is a hybrid quantum-classical algorithm because the preparation of the target state (2) involves applying quantum unitary gates, while the optimization of the cost function (3) can be achieved via conventional, classical means.

It is clear that the optimal solution found from  $\text{QAOA}_{p+1}$  is always better than that of  $\text{QAOA}_p$ . Moreover, for large  $p$  the QAOA can approximate the QAA via Trotterization. Since QAA can achieve with arbitrary accuracy the target ground state for any finite-size system if the speed of traversal is vanishingly small, this means that the QAOA can also produce with arbitrary accuracy any target ground state in the limit  $p \rightarrow \infty$ . However, for all practical purposes (small  $p$ ), the correspondence between the QAOA and QAA is not so clear, and thus in what follows we explore how well the QAOA can target certain hard-to-prepare quantum many-body states beyond those for which it was originally envisioned.

*GHZ state.* – Consider the 1d Hamiltonian with Ising interactions

$$H_I = -\sum_{i=1}^L Z_i Z_{i+1} \quad (4)$$

with periodic boundary conditions, for which the GHZ state is the ground state, in the symmetry sector  $G = \prod_i^L X_i = 1$ . If we start with the polarized state  $|+\rangle$  which

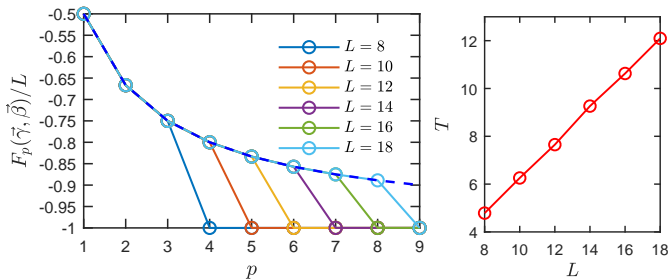


Figure 2. Preparation of GHZ state. (Left) Optimal cost function (3). One sees that  $F_p(\vec{\gamma}, \vec{\beta})/L = -1$  for  $p \geq L/2$ ; in other words, the GHZ state is created with perfect fidelity using  $\text{QAOA}_{p \geq L/2}$ . We have also plotted a conjectured analytic expression  $-p/(p+1)$  (from [35]) for the optimal cost function as the dashed blue line. (Right) Total minimum time  $T = \sum_i^{p=L/2} (\gamma_i + \beta_i)$  required for the QAOA to produce the GHZ state with perfect fidelity using  $\text{QAOA}_{p=L/2}$ . The minimization is performed over all the numerical solutions found. One sees a linear trend  $t \sim L$ .

has  $G = +1$ , then the QAOA protocol (2) respects this symmetry, and optimization of (3) as  $p \rightarrow \infty$  will necessarily yield the GHZ state, with  $\lim_{p \rightarrow \infty} F_p(\vec{\gamma}, \vec{\beta})/L \rightarrow -1$ .

We implement the QAOA, finding numerically the optimal angles  $(\vec{\gamma}_*, \vec{\beta}_*)$  that minimize (3) via a search by gradient descent of the parameter space  $\gamma_i, \beta_i \in [0, \pi/2)$  for all  $i$ , for system sizes  $L \leq L_1 = 18$ , and for  $p \leq L_1$ . We restrict each angle to be any contiguous interval of length  $\pi/2$  because  $e^{-i\frac{\pi}{2}H_I} \propto 1$  and  $e^{-i\frac{\pi}{2}H_X} \propto G$  which are conserved throughout the algorithm; furthermore, in order to give the set of angles  $(\vec{\gamma}, \vec{\beta})$  the interpretation of ‘time’, we choose  $\gamma_i, \beta_i \in [0, \pi/2)$ . We note that, for fixed  $L$ , assuming a fine mesh of each interval  $[0, \pi/2)$  into  $\mathcal{M}$  points, a brute force search of this parameter space takes an exponentially long time  $t \sim O(\mathcal{M}^{2p})$  in  $p$ . Consequently, we have ensured that the total number of runs performed is large enough to ensure convergence of the search algorithm to the global minimum.

Fig. 2 shows the results. We see that interestingly, the GHZ can be prepared with *perfect* fidelity, to machine precision, using the protocol  $\text{QAOA}_{p=L/2}$ , which has depth  $2p = L$ . This claim was stated in [43], though justified explicitly for  $p = 1$  only. We note that there are multiple optimal solutions for  $(\vec{\gamma}, \vec{\beta})$  that give this perfect fidelity. Since each angle  $\gamma_i, \beta_i$  is bounded from above, our numerical results imply that the time needed to prepare the GHZ state in a system of size  $L$  scales as  $t \sim O(L)$ . Indeed, in fig. 2, we see that the *minimum* amount of time  $T = \sum_i^{p=L/2} (\gamma_i + \beta_i)$  amongst all the solutions that we numerically found, at  $p = L/2$ , gives an almost perfect linear trend (See [44] for the explicit optimal angles). For each solution at every depth  $p$ , the vector of angles is symmetric under the reflection

$\gamma_i \leftrightarrow \beta_{L-i+1}$ ; this is due to the Kramers-Wannier duality of the Ising model which relates the paramagnet (product state) and the ferromagnet (GHZ).

The duality is manifest when rewritten in terms of Majorana fermions, which in turn provides a simple analytic route for preparing the GHZ state (and later, the toric code ground state) in a manner complementary to the QAOA scheme. Each spin corresponds via Jordan-Wigner transformation to two Majoranas fermions:  $\gamma_{2j-1} = Y_j \prod_{i=1}^{j-1} X_i$ ,  $\gamma_{2j} = Z_j \prod_{i=1}^{j-1} X_i$  for  $j$  ranging from 1 to  $L$ . Then  $X_j = -i\gamma_{2j-1}\gamma_{2j}$  and  $Z_j Z_{j+1} = i\gamma_{2j}\gamma_{2j+1}$ ; the product state and GHZ state simply correspond to the two different dimerization patterns of Majoranas. To transform from the state with all  $i\gamma_{2j-1}\gamma_{2j} = -1$  to the state with all  $i\gamma_{2j}\gamma_{2j+1} = +1$ , we need to sequentially exchange Majoranas pairwise ( $\gamma_1 \leftrightarrow \gamma_2, \gamma_2 \leftrightarrow \gamma_3, \dots$ ).  $S = e^{\frac{i\pi}{4}\gamma_i\gamma_j}$  is the SWAP operator which accomplishes each exchange:  $S^{-1}\gamma_{i,j}S = \mp\gamma_{j,i}$ . Thus,  $U$  is a product of successive SWAPs, which in the spin language is

$$U = \left( \prod_{i=1}^{L-1} e^{\frac{i\pi}{4}X_{i+1}} e^{\frac{i\pi}{4}Z_i Z_{i+1}} \right) e^{\frac{i\pi}{4}X_1}. \quad (5)$$

As the last operator (when acting on  $\otimes |X = 1\rangle$ ) contributes an overall phase and can be neglected, we have analytically found a depth  $2(L-1)$  circuit relating GHZ and product states exactly (see fig. 1a); this complements QAOA circuit discussed earlier. We note that such SWAPs were used in [45] to transform a product state into the ground state of the Kitaev chain.

*Critical state.* – Next let us consider the preparation of a critical state, namely the ground state of the 1d transverse field Ising model (TFIM)

$$H_{\text{TFIM}} = -\sum_{i=1}^L Z_i Z_{i+1} - \sum_{i=1}^L X_i \quad (6)$$

with periodic boundary conditions. We use a variant of the QAOA protocol: we employ the protocol (2) with  $H_I$  still given by (4), but instead evaluate the cost function (3) with  $H_{\text{TFIM}}$  in place of  $H_I$ . To benchmark the algorithm, we compute the many-body overlap  $|\langle \psi_t | \psi \rangle_p|^2$  of the prepared state  $|\psi\rangle_p$  with the corresponding target state  $|\psi_t\rangle$  (the ground state of (6) obtained by exact diagonalization of chains of size  $L$ ).

Figs. 3 show the results (see [44] for energy optimization plots and explicit optimal angles). Surprisingly, the critical state  $|\psi_t\rangle$  can also be prepared with *perfect* fidelity, to machine precision, using  $\text{QAOA}_{p=L/2}$ , which has depth  $2p = L$ , just like the GHZ case. This implies once again that the time needed to prepare a critical state of a system of size  $L$ , exactly, scales as  $t \sim O(L)$ .

The perfect fidelities achieved for both the GHZ and critical cases suggest that an analytic understanding of the result may be possible. However, while the model and

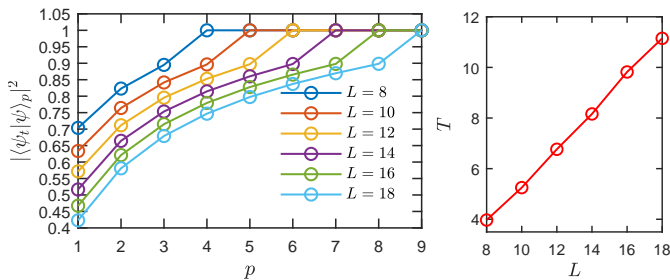


Figure 3. Preparation of critical state. (Left) Many-body overlap  $|\langle \psi_t | \psi \rangle_p|^2$  of the prepared state with the target ground state of (6) found by exact diagonalization. One sees perfect fidelity for  $p \geq L/2$ . (Right) Total minimum time  $T = \sum_{i=1}^{p=L/2} (\gamma_i + \beta_i)$  required for the QAOA to produce the critical state with perfect fidelity using  $\text{QAOA}_{p=L/2}$ . One sees a linear trend  $t \sim L$ .

unitary gates can be mapped to free fermions [43], the QAOA algorithm maps to a nonlinear optimization problem involving an extensive number of variables, which is highly nontrivial.

In fact, we conjecture that, for a one-dimensional system of even  $L$  spin-1/2s with periodic boundary conditions, any state produced by  $\text{QAOA}_p$  (2) for arbitrary  $p$  using  $H_I = -\sum_{i=1}^L Z_i Z_{i+1}$  and  $H_X = -\sum_{i=1}^L X_i$ , can also be achieved perfectly by  $\text{QAOA}_{p=L/2}$ , the protocol at  $p = L/2$ . This would imply that we can achieve the ground state of the TFIM at any point in the phase diagram using  $\text{QAOA}_{p=L/2}$ , which in particular would cover the GHZ and critical cases. In [44], we provide extra details and numerical evidence to support this conjecture.

*Ground state of the Toric code.* – Finally, we consider the preparation of a topologically ordered state, specifically the ground state of the  $\mathbb{Z}_2$  Wen-plaquette model, which is unitarily equivalent to the Kitaev toric code. Let us write the Pauli matrices  $(X, Y, Z)$  as  $(\sigma^x, \sigma^y, \sigma^z)$ . The Hamiltonian is given by

$$H_I = -\sum_{i=1}^L \sum_{j=1}^L \sigma_{i,j+1}^x \sigma_{i+1,j+1}^y \sigma_{i+1,j}^x \sigma_{i,j}^y, \quad (7)$$

where we have assumed periodic boundary conditions and even  $L$ . We find analytically a depth- $2(L-1)$  circuit which exactly produces the ground state of the Wen plaquette model from a product state, and we also show that the protocol  $\text{QAOA}_{p=L/2}$  of depth  $2p = L$  achieves this result. This implies that surprisingly, the time needed to prepare the toric code ground state using this approach scales as  $t \sim O(L)$ , a lower bound derived in [41]. (See [46] for a very different approach for preparing surface code states).

We first use the analytic circuit preparing GHZ state, described in the above corresponding section, to construct an analytic circuit preparing a ground state of

the Wen-plaquette model (7). The goal is to transform the (product) state stabilized by  $-\sum_{i=1}^L \sum_{j=1}^L \sigma_{i,j}^x$  to the topologically ordered state stabilized by  $H_I$  and the two logical operators  $L_1 = \prod_{i=1}^L \sigma_{i,i}^x$  and  $L_2 = \prod_{i=1}^L \sigma_{i,i+1}^x$ .

We can map operators which act within a subspace of the original  $\sigma$  variables to a dual set of operators. Define the subspace  $\mathcal{H}_S$  to be the original Hilbert space subject to the  $L$  constraints  $\prod_{i=1}^L \sigma_{i,j}^x = 1$  for  $j = 1, \dots, L$ ;  $\mathcal{H}_S$  has dimension  $2^{L^2-L}$ .

We will define a new set of Pauli operators  $\tau$  residing on the centers of plaquettes (this dual set of variables was exploited in [47] for different purposes);  $\tau_{i,j}$  is located on the center of the plaquette with lower left corner at  $(i, j)$ . All operators preserving  $\mathcal{H}_S$  (commuting with the constraints) can be rewritten in terms of  $\tau$  operators via the following dictionary:

$$\begin{aligned} \tau_{i,j}^x &= \sigma_{i,j+1}^x \sigma_{i+1,j+1}^y \sigma_{i+1,j}^x \sigma_{i,j}^y, \\ \tau_{i,j}^z \tau_{i+1,j+1}^z &= \sigma_{i+1,j+1}^x, \end{aligned} \quad (8)$$

and the  $\tau$  operators are subject to the  $L$  constraints  $\prod_{i=1}^L \tau_{i,j}^x = 1$  for  $j = 1, \dots, L$ . It is straightforward to check that the constrained  $\tau$  operators as defined above satisfy the same algebra and constraints as the constrained  $\sigma$  operators.

Thus, for each diagonal (labeled  $j$ ) of  $\tau$  spins, we simply use the (inverse) GHZ printing circuit (5) to transform the state stabilized by

$$\{-\tau_{i,j}^z \tau_{i+1,j+1}^z = -\sigma_{i+1,j+1}^x\}_{i=1}^L \quad (9)$$

and  $\prod_{i=1}^L \tau_{i,j}^x = 1$  into the state stabilized by

$$\{-\tau_{i,j}^x = -\sigma_{i,j+1}^x \sigma_{i+1,j+1}^y \sigma_{i+1,j}^x \sigma_{i,j}^y\}_{i=1}^L, \quad (10)$$

which can be done in parallel as all operators on a diagonal commute with all operators on other diagonals (see fig. 1b). In doing so, the ground state of the toric code is prepared. Moreover, note that the logical operator  $(L_1, L_2)$  constraints are preserved at all steps of the circuit.

We have analytically found depth  $2(L-1)$  circuits preparing the GHZ and toric code ground states, and these circuits are qualitatively different from QAOA circuits, which act on all degrees of freedom in a single layer of the circuit. However, as we have shown, preparing the toric code ground state simply involves parallelizing the preparation of GHZ states. Since there exists an application of the algorithm  $\text{QAOA}_{p=L/2}$  that prepares the GHZ state, these parameters can thus be used to construct a QAOA circuit of depth  $2p = L$  that prepares the toric code ground state perfectly. In [44], we numerically verify that this is indeed true.

*Discussion and conclusion.* – We have provided explicit, efficient unitary circuits which can prepare, with perfect fidelity, nontrivial states (GHZ, critical, and

topologically ordered) from unentangled product states. Practically, such circuits are readily applicable to synthetic quantum systems such as trapped ions and superconducting qubits, and such non-trivial state preparation is useful for both quantum metrology and simulations (an important question we have addressed in [44] is the effect of imperfect sequences on state preparation). For example, the non-trivial entanglement structure of these states could be directly measured by preparing multiple copies of the states and using recently developed protocols [48, 49]. It would be interesting to extract the central charge of the critical system or topological entanglement entropy of the toric code state. Furthermore, truncating the analytic circuit at intermediate depth allows one to prepare a state with a boundary separating toric code and a trivial paramagnet.

More generally, our studies illustrate that QAOA variational wavefunctions can capture even non-trivial phases of matter beyond which the algorithm was designed for. We have targeted non-trivial fixed point wavefunctions (with either zero or infinite correlation length), in integrable systems. The next step is to target more general ground states of interacting Hamiltonians. As moving within phases is simpler (requiring only finite depth circuits) than crossing phase boundaries, we expect that QAOA can efficiently accommodate the more general cases, though without perfect fidelity. In addition to providing practical circuits and variational wavefunctions, QAOA is a potential tool for addressing questions of complexity of a ground state. In the examples provided, it furnishes circuits with minimal depth scaling with size and may offer valuable guidance in determining the circuit complexity [50–52] needed to prepare various states of matter.

*Acknowledgments.* – We thank Daniel Gottesman, Gábor Halász, Germán Sierra, Romain Vasseur, Soonwon Choi, Shengtao Wang, and Valentin Kasper for useful discussions. WWH and THH are supported by the Gordon and Betty Moore Foundations EPiQS Initiative through Grant No. GBMF4306 and Grant No. GBMF4304.

- 
- [1] R. Blatt and C. F. Roos, “Quantum simulations with trapped ions,” *Nature Physics* **8**, 277–284 (2012).
- [2] J. Zhang, G. Pagano, P. W. Hess, A. Kyprianidis, P. Becker, H. Kaplan, A. V. Gorshkov, Z.-X. Gong, and C. Monroe, “Observation of a many-body dynamical phase transition with a 53-qubit quantum simulator,” *Nature* **551**, 601 EP – (2017).
- [3] Hannes Bernien, Sylvain Schwartz, Alexander Keesling, Harry Levine, Ahmed Omran, Hannes Pichler, Soonwon Choi, Alexander S. Zibrov, Manuel Endres, Markus Greiner, Vladan Vuletic, and Mikhail D. Lukin, “Probing many-body dynamics on a 51-atom quantum simulator,” *Nature* **551**, 579 EP – (2017), article.
- [4] Immanuel Bloch, Jean Dalibard, and Wilhelm Zwerger, “Many-body physics with ultracold gases,” *Rev. Mod. Phys.* **80**, 885–964 (2008).
- [5] R. Barends, J. Kelly, A. Megrant, D. Sank, E. Jeffrey, Y. Chen, Y. Yin, B. Chiaro, J. Mutus, C. Neill, P. O’Malley, P. Roushan, J. Wenner, T. C. White, A. N. Cleland, and John M. Martinis, “Coherent josephson qubit suitable for scalable quantum integrated circuits,” *Phys. Rev. Lett.* **111**, 080502 (2013).
- [6] Jay M. Gambetta, Jerry M. Chow, and Matthias Steffen, “Building logical qubits in a superconducting quantum computing system,” *npj Quantum Information* **3**, 2 (2017).
- [7] M. Aidelsburger, M. Atala, M. Lohse, J. T. Barreiro, B. Paredes, and I. Bloch, “Realization of the hofstadter hamiltonian with ultracold atoms in optical lattices,” *Phys. Rev. Lett.* **111**, 185301 (2013).
- [8] Gregor Jotzu, Michael Messer, Rémi Desbuquois, Martin Lebrat, Thomas Uehlinger, Daniel Greif, and Tilman Esslinger, “Experimental realization of the topological haldane model with ultracold fermions,” *Nature* **515**, 237 EP – (2014).
- [9] M. Aidelsburger, M. Lohse, C. Schweizer, M. Atala, J.T. Barreiro, S. Nascimbène, N. R. Cooper, I. Bloch, and N. Goldman, “Measuring the chern number of hofstadter bands with ultracold bosonic atoms,” *Nature Physics* **11**, 162 EP – (2014).
- [10] Markus Greiner, Olaf Mandel, Tilman Esslinger, Theodor W. Hänsch, and Immanuel Bloch, “Quantum phase transition from a superfluid to a mott insulator in a gas of ultracold atoms,” *Nature* **415**, 39 EP – (2002), article.
- [11] Jae-yoon Choi, Sebastian Hild, Johannes Zeiher, Peter Schauß, Antonio Rubio-Abadal, Tarik Yefsah, Vedika Khemani, David A. Huse, Immanuel Bloch, and Christian Gross, “Exploring the many-body localization transition in two dimensions,” *Science* **352**, 1547–1552 (2016).
- [12] Michael Schreiber, Sean S. Hodgman, Pranjal Bordia, Henrik P. Lüschen, Mark H. Fischer, Ronen Vosk, Ehud Altman, Ulrich Schneider, and Immanuel Bloch, “Observation of many-body localization of interacting fermions in a quasirandom optical lattice,” *Science* **349**, 842–845 (2015).
- [13] G. Kucsko, S. Choi, J. Choi, P. C. Maurer, H. Sumiya, S. Onoda, J. Isoya, F. Jelezko, E. Demler, N. Y. Yao, and M. D. Lukin, “Critical thermalization of a disordered dipolar spin system in diamond,” ArXiv e-prints (2016), [arXiv:1609.08216 \[cond-mat.mes-hall\]](https://arxiv.org/abs/1609.08216).
- [14] J. Zhang, P. W. Hess, A. Kyprianidis, P. Becker, A. Lee, J. Smith, G. Pagano, I.-D. Potirniche, A. C. Potter, A. Vishwanath, N. Y. Yao, and C. Monroe, “Observation of a discrete time crystal,” *Nature* **543**, 217–220 (2017).
- [15] Soonwon Choi, Joonhee Choi, Renate Landig, Georg Kucsko, Hengyun Zhou, Junichi Isoya, Fedor Jelezko, Shinobu Onoda, Hitoshi Sumiya, Vedika Khemani, Curt von Keyserlingk, Norman Y. Yao, Eugene Demler, and Mikhail D. Lukin, “Observation of discrete time-crystalline order in a disordered dipolar many-body system,” *Nature* **543**, 221–225 (2017).
- [16] J. Smith, A. Lee, P. Richerme, B. Neyenhuis, P. W. Hess, P. Hauke, M. Heyl, D. A. Huse, and C. Monroe, “Many-body localization in a quantum simulator with programmable random disorder,” *Nature Physics* **12**, 907

- EP – (2016).
- [17] D. Leibfried, M. D. Barrett, T. Schaetz, J. Britton, J. Chiaverini, W. M. Itano, J. D. Jost, C. Langer, and D. J. Wineland, “Toward heisenberg-limited spectroscopy with multiparticle entangled states,” *Science* **304**, 1476–1478 (2004).
- [18] Vittorio Giovannetti, Seth Lloyd, and Lorenzo Maccone, “Quantum-enhanced measurements: Beating the standard quantum limit,” *Science* **306**, 1330–1336 (2004).
- [19] C. L. Degen, F. Reinhard, and P. Cappellaro, “Quantum sensing,” *Rev. Mod. Phys.* **89**, 035002 (2017).
- [20] S. Choi, N. Y. Yao, and M. D. Lukin, “Quantum metrology based on strongly correlated matter,” ArXiv e-prints (2018), [arXiv:1801.00042](https://arxiv.org/abs/1801.00042) [quant-ph].
- [21] Robert Raussendorf, Daniel E. Browne, and Hans J. Briegel, “Measurement-based quantum computation on cluster states,” *Phys. Rev. A* **68**, 022312 (2003).
- [22] H. J. Briegel, D. E. Browne, W. Dür, R. Raussendorf, and M. Van den Nest, “Measurement-based quantum computation,” *Nature Physics* **5**, 19 EP – (2009).
- [23] B. P. Lanyon, P. Jurcevic, M. Zwerger, C. Hempel, E. A. Martinez, W. Dür, H. J. Briegel, R. Blatt, and C. F. Roos, “Measurement-based quantum computation with trapped ions,” *Phys. Rev. Lett.* **111**, 210501 (2013).
- [24] E. Farhi, J. Goldstone, S. Gutmann, and M. Sipser, “Quantum Computation by Adiabatic Evolution,” eprint [arXiv:quant-ph/0001106](https://arxiv.org/abs/quant-ph/0001106) (2000), [quant-ph/0001106](https://arxiv.org/abs/quant-ph/0001106).
- [25] Edward Farhi, Jeffrey Goldstone, Sam Gutmann, Joshua Lapan, Andrew Lundgren, and Daniel Preda, “A quantum adiabatic evolution algorithm applied to random instances of an np-complete problem,” *Science* **292**, 472–475 (2001).
- [26] Mustafa Demirplak and Stuart A. Rice, “Adiabatic population transfer with control fields,” *The Journal of Physical Chemistry A* **107**, 9937–9945 (2003), <https://doi.org/10.1021/jp030708a>.
- [27] Mustafa Demirplak and Stuart A. Rice, “Assisted adiabatic passage revisited,” *The Journal of Physical Chemistry B* **109**, 6838–6844 (2005), PMID: 16851769, <https://doi.org/10.1021/jp040647w>.
- [28] M V Berry, “Transitionless quantum driving,” *Journal of Physics A: Mathematical and Theoretical* **42**, 365303 (2009).
- [29] Dries Sels and Anatoli Polkovnikov, “Minimizing irreversible losses in quantum systems by local counterdiabatic driving,” *Proceedings of the National Academy of Sciences* (2017), [10.1073/pnas.1619826114](https://doi.org/10.1073/pnas.1619826114).
- [30] L.S. Pontryagin, *Mathematical Theory of Optimal Processes* (1987).
- [31] Robert F. Stengel, *Optimal Control and Estimation* (1994).
- [32] Constantin Brif, Matthew D Grace, Mohan Sarovar, and Kevin C Young, “Exploring adiabatic quantum trajectories via optimal control,” *New Journal of Physics* **16**, 065013 (2014).
- [33] Zhi-Cheng Yang, Armin Rahmani, Alireza Shabani, Hartmut Neven, and Claudio Chamon, “Optimizing variational quantum algorithms using pontryagin’s minimum principle,” *Phys. Rev. X* **7**, 021027 (2017).
- [34] Note there have also been works that depart from the working principle of adiabaticity but are not bang-bang in nature: for example one can perform a specially designed quantum quench in space that minimizes the generation of excitations behind the quench front [53].
- [35] E. Farhi, J. Goldstone, and S. Gutmann, “A Quantum Approximate Optimization Algorithm,” ArXiv e-prints (2014), [arXiv:1411.4028](https://arxiv.org/abs/1411.4028) [quant-ph].
- [36] E. Farhi and A. W Harrow, “Quantum Supremacy through the Quantum Approximate Optimization Algorithm,” ArXiv e-prints (2016), [arXiv:1602.07674](https://arxiv.org/abs/1602.07674) [quant-ph].
- [37] Dave Wecker, Matthew B. Hastings, and Matthias Troyer, “Progress towards practical quantum variational algorithms,” *Phys. Rev. A* **92**, 042303 (2015).
- [38] M. B. Hastings, “Locality in Quantum Systems,” ArXiv e-prints (2010), [arXiv:1008.5137](https://arxiv.org/abs/1008.5137) [math-ph].
- [39] Alexei Kitaev and John Preskill, “Topological entanglement entropy,” *Phys. Rev. Lett.* **96**, 110404 (2006).
- [40] Michael Levin and Xiao-Gang Wen, “Detecting topological order in a ground state wave function,” *Phys. Rev. Lett.* **96**, 110405 (2006).
- [41] S. Bravyi, M. B. Hastings, and F. Verstraete, “Lieb-robinson bounds and the generation of correlations and topological quantum order,” *Phys. Rev. Lett.* **97**, 050401 (2006).
- [42] C-M. Jian, I.H. Kim, and X-L. Qi, “Long-range mutual information and topological uncertainty principle,” ArXiv e-prints (2015), [arXiv:1508.07006](https://arxiv.org/abs/1508.07006) [cond-mat.str-el].
- [43] Zhihui Wang, Stuart Hadfield, Zhang Jiang, and Eleanor G. Rieffel, “Quantum approximate optimization algorithm for maxcut: A fermionic view,” *Phys. Rev. A* **97**, 022304 (2018).
- [44] See supplemental information.
- [45] Yichen Huang and Xie Chen, “Quantum circuit complexity of one-dimensional topological phases,” *Phys. Rev. B* **91**, 195143 (2015).
- [46] Eric Dennis, Alexei Kitaev, Andrew Landahl, and John Preskill, “Topological quantum memory,” *Journal of Mathematical Physics* **43**, 4452–4505 (2002), <https://doi.org/10.1063/1.1499754>.
- [47] Jing Yu, Su-Peng Kou, and Xiao-Gang Wen, “Topological quantum phase transition in the transverse wenzelquette model,” *EPL (Europhysics Letters)* **84**, 17004 (2008).
- [48] Dmitry A. Abanin and Eugene Demler, “Measuring entanglement entropy of a generic many-body system with a quantum switch,” *Phys. Rev. Lett.* **109**, 020504 (2012).
- [49] Rajibul Islam, Ruichao Ma, Philipp M. Preiss, M. Eric Tai, Alexander Lukin, Matthew Rispoli, and Markus Greiner, “Measuring entanglement entropy in a quantum many-body system,” *Nature* **528**, 77 EP – (2015), article.
- [50] Michael A. Nielsen, “A geometric approach to quantum circuit lower bounds,” *Quantum Info. Comput.* **6**, 213–262 (2006).
- [51] L. Susskind, “Entanglement is not enough,” ArXiv e-prints (2014), [arXiv:1411.0690](https://arxiv.org/abs/1411.0690) [hep-ph].
- [52] Robert A. Jefferson and Robert C. Myers, “Circuit complexity in quantum field theory,” *Journal of High Energy Physics* **2017**, 107 (2017).
- [53] K. Agarwal, R. N. Bhatt, and S. L. Sondhi, “Fast preparation of critical ground states using superluminal fronts,” ArXiv e-prints (2017), [arXiv:1710.09840](https://arxiv.org/abs/1710.09840) [cond-mat.quant-gas].

## SUPPLEMENTAL INFORMATION

### Appendix A. Optimal angles for preparing GHZ state at $p = L/2$

The following are the numerically found optimized set of angles  $(\gamma_1, \beta_1, \dots, \gamma_{p=L/2}, \beta_{p=L/2})$  employed by QAOA $_{p=L/2}$  which produce the GHZ state with perfect fidelity at various system sizes and with least amount of time  $T = \sum_i^{p=L/2} (\gamma_i + \beta_i)$ .

$L = 8, T = 4.7867 :$

$$(0.5297, 0.5243, 0.7243, 0.6151, \\ 0.6151, 0.7243, 0.5243, 0.5297) \quad (11)$$

$L = 10, T = 6.257:$

$$(0.5814, 0.5230, 0.6360, 0.7889, 0.5993, \\ 0.5993, 0.7889, 0.6360, 0.5230, 0.5814) \quad (12)$$

$L = 12, T = 7.651:$

$$(0.5466, 0.5452, 0.6902, 0.7212, 0.5946, 0.7276 \\ 0.7276, 0.5946, 0.7212, 0.6902, 0.5452, 0.5466) \quad (13)$$

$L = 14, T = 9.2634:$

$$(0.6513, 0.5696, 0.5841, 0.6704, 0.7633, \\ 0.8270, 0.5660, 0.5660, 0.8270, \\ 0.7633, 0.6704, 0.5841, 0.5696, 0.6513) \quad (14)$$

$L = 16, T = 10.6273:$

$$(0.5846, 0.5796, 0.6105, 0.7155, \\ 0.7966, 0.6152, 0.6373, 0.7745, \\ 0.7745, 0.6373, 0.6152, 0.7966, \\ 0.7155, 0.6105, 0.5796, 0.5846) \quad (15)$$

$L = 18, T = 12.096:$

$$(0.6064, 0.5232, 0.6632, 0.7780, 0.6660, \\ 0.6302, 0.7773, 0.7133, 0.6904, \\ 0.6904, 0.7133, 0.7773, 0.6302, \\ 0.6660, 0.7780, 0.6632, 0.5232, 0.6064) \quad (16)$$

### Appendix B. Energy optimization plot and optimal angles for preparing critical state at $p = L/2$

In Fig. 4 we present the optimal cost function given by the energy of the TFIM,

$$F_p(\vec{\gamma}, \vec{\beta}) = {}_p \langle \psi(\vec{\gamma}, \vec{\beta}) | H_{\text{TFIM}} | \psi(\vec{\gamma}, \vec{\beta}) \rangle_p, \quad (17)$$

used in the preparation of the critical state.

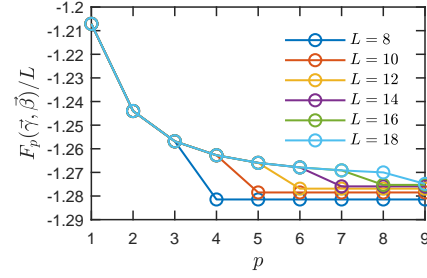


Figure 4. Preparation of critical state. Optimal cost function (17) with energy as measured by the TFIM Hamiltonian.

The following are the numerically found optimized set of angles  $(\gamma_1, \beta_1, \dots, \gamma_{p=L/2}, \beta_{p=L/2})$  employed by QAOA $_{p=L/2}$  which produce the critical state with perfect fidelity at various system sizes and with least amount of time  $T = \sum_i^{p=L/2} (\gamma_i + \beta_i)$ .

$L = 8, T = 3.9699 :$

$$(0.2496, 0.6845, 0.4808, 0.6559 \\ 0.5260, 0.6048, 0.4503, 0.3180) \quad (18)$$

$L = 10, T = 5.250:$

$$(0.2473, 0.6977, 0.4888, 0.6783, 0.5559, \\ 0.6567, 0.5558, 0.6029, 0.4598, 0.3068) \quad (19)$$

$L = 12, T = 6.7651:$

$$(0.2809, 0.6131, 0.6633, 0.4537, 0.8653, 0.4663, \\ 0.6970, 0.6829, 0.4569, 0.7990, 0.3565, 0.4304) \quad (20)$$

$L = 14, T = 8.1604:$

$$(0.3090, 0.5710, 0.6923, 0.5648, 0.5391, \\ 0.9684, 0.3979, 0.6852, 0.8235, \\ 0.4474, 0.6930, 0.6465, 0.4120, 0.4104) \quad (21)$$

$L = 16, T = 9.8198:$

$$(0.3790, 0.5622, 0.5638, 0.7101, \\ 0.9046, 0.3210, 0.6738, 0.8377, \\ 0.8616, 0.4004, 0.5624, 0.9450, \\ 0.5224, 0.6466, 0.4119, 0.5172) \quad (22)$$

$L = 18, T = 11.1485:$

$$(0.3830, 0.4931, 0.7099, 0.7010, 0.5330, \\ 0.6523, 0.6887, 1.0405, 0.3083, \\ 0.6215, 0.9607, 0.5977, 0.6209, \\ 0.5597, 0.7850, 0.5851, 0.4132, 0.4948) \quad (23)$$

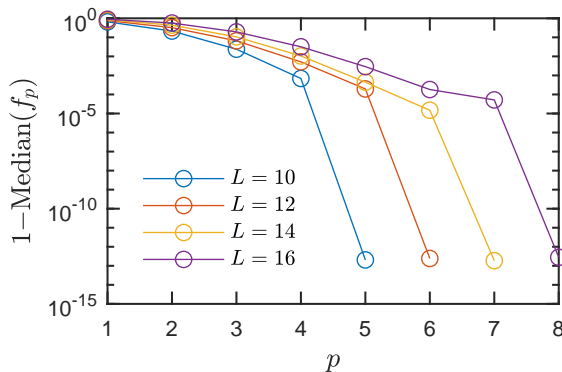


Figure 5. Typical optimal infidelity of  $\text{QAOA}_p$  for  $1 \leq p \leq L/2$  used to target a random state produced by  $\text{QAOA}_{p=L/2+1}$  (given by the median over 5000 realizations of random states). One sees a clear dip at  $p = L/2$ , to a value close to machine precision (which we take to be  $\sim 10^{-13}$ ), indicating that the  $\text{QAOA}_{p=L/2}$  is able to target a random state with perfect fidelity typically.

### Appendix C: A Conjecture and Numerical Support

Consider a one-dimensional system of an even number  $L$  spin-1/2s with periodic boundary conditions, and consider  $H_I = -\sum_{i=1}^L Z_i Z_{i+1}$  and  $H_X = -\sum_i X_i$ . Our conjecture is that any state produced by a  $\text{QAOA}_p$  protocol of arbitrary depth  $p$  can be obtained by  $\text{QAOA}_{p=L/2}$ . In other words, for any depth  $p$  and set of angles  $(\vec{\gamma}, \vec{\beta}) \equiv (\gamma_1, \dots, \gamma_p, \beta_1, \dots, \beta_p)$ , there exists a set of angles  $(\vec{\gamma}', \vec{\beta}') \equiv (\gamma'_1, \dots, \gamma'_{L/2}, \beta'_1, \dots, \beta'_{L/2})$  such that

$$e^{-i\beta'_{L/2} H_X} e^{-i\gamma'_{L/2} H_I} \dots e^{-i\beta'_1 H_X} e^{-i\gamma'_1 H_I} |+\rangle \quad (24)$$

$$= e^{-i\beta_p H_X} e^{-i\gamma_p H_I} \dots e^{-i\beta_1 H_X} e^{-i\gamma_1 H_I} |+\rangle. \quad (25)$$

It suffices to establish this result for  $p = L/2 + 1$ , because one could then contract the depth  $2p = 2(L/2 + 1)$  unitary into a depth  $2p = L$  unitary, and iterate this process to achieve a total depth  $2p = L$ . We have tested this result for different system sizes by generating random states  $|\psi^{(r)}(\vec{\gamma}, \vec{\beta})\rangle_{L/2+1}$  produced using the  $\text{QAOA}_{p=L/2+1}$  protocol with random angles  $(\gamma_1, \dots, \gamma_{L/2+1}, \beta_1, \dots, \beta_{L/2+1})$ , and targeting them using the protocol  $\text{QAOA}_p$  for  $p$  up to  $L/2$ . More precisely, given a random state  $|\psi^{(r)}(\vec{\gamma}, \vec{\beta})\rangle_{L/2+1}$ , we maximize the fidelity

$$f_p(\vec{\gamma}', \vec{\beta}') = \left| \langle \psi(\vec{\gamma}', \vec{\beta}') | \psi^{(r)}(\vec{\gamma}, \vec{\beta}) \rangle_{L/2+1} \right|^2, \quad (26)$$

over  $(\vec{\gamma}', \vec{\beta}')$ , where  $|\psi(\vec{\gamma}', \vec{\beta}')\rangle_p$  is the state produced by  $\text{QAOA}_p$ .

Figs. 5, 6 show the results. In fig. 5, we plot the typical optimal infidelity  $1 - \text{Median}(f_p)$ , given by the median

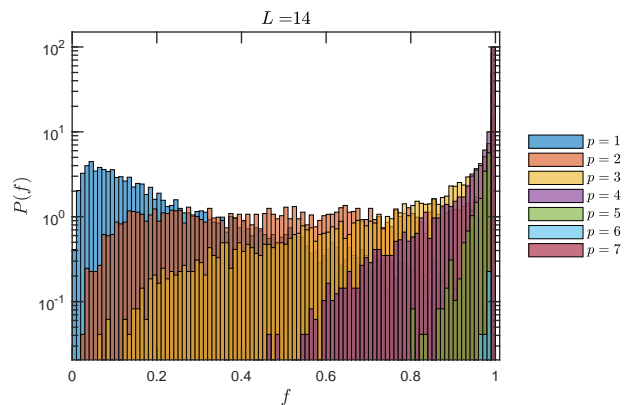


Figure 6. Probability distribution of optimal fidelities, for system size  $L = 14$ . For  $p = L/2$ , the optimal fidelities are singularly peaked at  $f = 1$ , indicating that *all* instances of random states produced by  $\text{QAOA}_{p=L/2+1}$  can be targeted using  $\text{QAOA}_{p=L/2}$  perfectly; this is in contrast to  $p < L/2$  where there is some spread in the distribution, indicating that there are instances of random states for which  $\text{QAOA}_{p < L/2}$  cannot target them. Probability distributions for other system sizes is qualitatively similar to one shown here.

over all realizations of random states (we have used 5000 random states and ensured convergence of the algorithm to the global minimum) against  $p$ , and for various  $L$ s. We see that a typical run of  $\text{QAOA}_p$  for  $p = L/2$  is able to target the input state  $|\psi^{(r)}(\vec{\gamma}, \vec{\beta})\rangle_{L/2+1}$  with perfect fidelity (to machine precision), while not for  $p < L/2$ . The reason we do not use the mean value, is because this undesirably overly weights the contributions of numerical imprecisions in the optimization algorithm. However, to make a statement about whether  $\text{QAOA}_{p=L/2}$  is able to *always* reach the target random state, we need to analyze the full *distribution* of the optimal fidelities. In fig. 6, we plot the *distribution* of the optimal fidelities for one of the system sizes considered and for various  $p$ s by plotting the probability distributions  $P(f)$  of the optimal fidelities  $f$ . We find that at  $p = L/2$ , the distribution is singularly peaked at  $f = 1$  (to machine precision), indicating that in fact, *all* realizations of random states created using  $\text{QAOA}_{p=L/2+1}$  can be targeted with  $\text{QAOA}_{p=L/2}$ , perfectly. This is in contrast to the optimal fidelities obtained for  $p < L/2$ : there is some spread in the distributions, indicating that there are instances of random states for which  $\text{QAOA}_{p < L/2}$  cannot reproduce it. Thus, our numerics gives support to the conjecture that any state produced using  $\text{QAOA}_{p \geq L/2+1}$  can be obtained by  $\text{QAOA}_{p=L/2}$ .

One important consequence of the above conjecture is that the ground state of any point in the transverse field Ising model ( $H = H_I + gH_X$  for arbitrary  $g$ ) can be achieved with perfect fidelity by  $\text{QAOA}_{p=L/2}$ . This is because as the ansatz depth approaches infinity,  $\text{QAOA}$



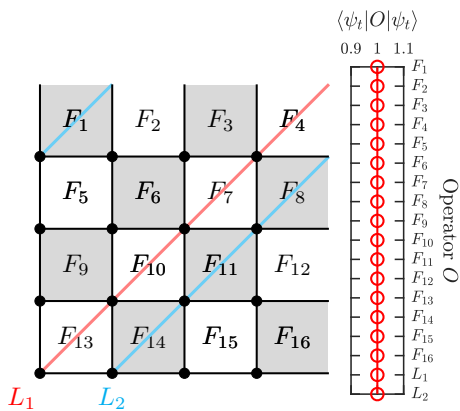


Figure 7. Numerical preparation of the Wen plaquette ground state using  $\text{QAOA}_{p=L/2}$ . Here  $L = 4$ , and we use the angles found from  $\text{QAOA}_2$  that produced the GHZ state. The left plot describes the geometry of the set-up, and illustrates the plaquette operators  $F_i$  which make up the Hamiltonian  $H = -\sum_i F_i$  as well as the two logical operators  $L_1$  and  $L_2$  which wrap around the torus. The right plot shows the expectation value of the plaquette operators and logical operators in the state prepared by QAOA. One sees that all expectation values are +1 to machine precision, indicating a perfect preparation of the ground state.

includes the trotterized adiabatic algorithm as a subset, and the latter can achieve any ground state in the phase diagram if infinite depth is permitted. Our conjecture then implies that such a circuit can be contracted to one of depth  $2p = L$ .

As for proving the conjecture, we note that leveraging the free fermion representation of the model, as done in [43], is a promising route. However, such a representation nonetheless involves a nonlinear (and hence nontrivial) optimization problem which we leave for future work.

#### Appendix D: Numerical verification of preparation of toric code ground state

We show here numerics that verify that we can prepare using  $\text{QAOA}_{p=L/2}$  the ground state of the Wen-plaquette model in the sector  $(L_1, L_2) = (+1, +1)$ , using the angles found previously of a  $\text{QAOA}_{p=L/2}$  circuit which prepared the GHZ state.

Fig. 7 shows the result for a  $L \times L$  Wen-plaquette model, where  $L = 4$  (so that there are only four angles  $(\gamma_1, \gamma_2, \beta_1, \beta_2)$  employed by the QAOA protocol). We see that all plaquette operators and logical operators carry a unit expectation value in the state prepared by the QAOA, which indicates that we can indeed prepare the ground state of the Wen-plaquette model in the appropriate logical sector as mentioned in the main text.

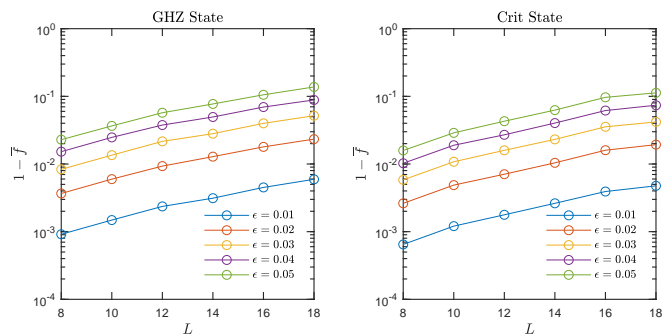


Figure 8. Effect of errors of strength  $\epsilon$  on the QAOA preparation of GHZ and critical states for system size  $L$ . Plotted is the infidelity averaged over 1000 error realizations (denoted by the overline).

Note that this circuit derived from QAOA is different from the analytic depth- $2(L-1)$  circuit (using SWAP operators) that also prepares the Wen-plaquette ground state exactly.

#### Appendix E: Effect of errors on QAOA state preparation

To probe the sensitivity of our state preparation protocol to imperfections, we introduced random errors to the optimal angles and calculated the resulting infidelity  $f = 1 - |\langle \psi_t | \psi \rangle_{L/2}|^2$  for  $\text{QAOA}_{p=L/2}$ , averaged over 1000 realizations of errors. Specifically, for each optimal angle  $\gamma_*$ , we introduce an error  $\gamma = \gamma_*(1 + \epsilon R)$ , where  $R$  is chosen randomly from the uniform distribution  $[-1, 1]$  and  $\epsilon$  parameterizes the strength of error (0.01, 0.02, 0.03, 0.04, or 0.05 in our study).

Fig. 8 shows the results for both the GHZ and critical states, for various system sizes and error strengths. Although the infidelity appears to increase exponentially with  $L$ , we see that for experimentally accessible system sizes (on the order of ten qubits), the infidelity is small ( $< 0.01$  infidelity for  $\epsilon = 0.01$  in  $L = 18$ ).